Available online at www.sciencedirect.com

SCIENCE DIRECT®

Earth and Planetary Science Letters 225 (2004) 205–220

EPSL

www.elsevier.com/locate/epsl

Intensification and variability of ocean thermohaline circulation through the last deglaciation

Alexander M. Piotrowski*, Steven L. Goldstein, Sidney R. Hemming, Richard G. Fairbanks

Lamont–Doherty Earth Observatory, Department of Earth and Environmental Sciences, Columbia University, Palisades, NY 10964, USA

Received 31 December 2003; received in revised form 28 May 2004; accepted 2 June 2004
Available online 27 July 2004
Editor: E. Bard

Abstract

Neodymium isotope ratios in the authigenic ferromanganese oxide component in a southeastern Atlantic core reveal a history of the global overturning circulation intensity through the last deglaciation. From a minimum during the Last Glacial Maximum (LGM), North Atlantic Deep Water (NADW) began to strengthen between 18 and 17 kyr cal. BP, approximately 2000–3000 years before the Bølling warming. It exhibits a gradually increasing baseline intensity that plateaus in the early Holocene, tracks increasing Northern Hemisphere insolation and parallels atmospheric CO_2 concentration. Millennial-scale fluctuations are superimposed on this baseline NADW increase, corresponding to events in Northern Hemisphere climate records. The millennial excursions show sharp increases associated with the pre-Bølling retreat of continental glaciers and the Bølling warming itself, a decrease with Allerød cooling, and a recovery through the Younger Dryas and early Holocene. The data confirm a close link between deep-ocean circulation and North Atlantic climate changes. There is no clear linkage with meltwater pulses, indicating that rapid meltwater additions did not trigger observable mode changes in NADW production. However, rapid changes in North Atlantic sea ice cover show a strong relationship with the millennial perturbations of NADW flux to the deep Southern Ocean. The data indicate that the baseline intensity of NADW reaching the Cape Basin is paced by Northern Hemisphere insolation and that North Atlantic sea ice coverage acts as a major amplifying link between the oceans and the atmosphere.

Keywords: thermohaline circulation; deep water; deglacial; neodymium; Younger Dryas; last glacial

1. Introduction

The role of deep ocean circulation in climate change has been a subject of intense debate. Abrupt changes observed in Northern Hemisphere climate records have been interpreted as a response to either rapid changes in North Atlantic Deep Water (NADW) production or reorganizations of atmospheric circulation [1–3]. The South Atlantic Ocean has been an important region for investigating changes in the global overturning circulation intensity because its proximity to the Circum-Antarctic allows sensitive monitoring of changes in proxy signals for NADW and circumpolar water.

* Corresponding author. Tel.: +1-845-365-8793; fax: +1-845-365-8155.
E-mail address: arcturus@ldeo.columbia.edu (A.M. Piotrowski).

0012-821X/$ - see front matter © 2004 Elsevier B.V. All rights reserved.
doi:10.1016/j.epsl.2004.06.002

The history of paleocirculation is currently still unresolved because different nutrient proxies used to trace paleo-water masses give conflicting results. Studies using benthic foraminiferal $\delta^{13}C$ have concluded that glacial NADW production was significantly weaker than today [4–6], while studies based on Cd/Ca and $^{231}Pa/^{230}Th$ ratios have concluded that NADW export to the Southern Ocean was equally robust during glacial and interglacial periods [7–9]. However, the circulation signal of these proxies can be overwritten by secondary effects such as regional air–sea exchange [10,11], biological productivity changes [12], dissolution of foraminiferal calcite [13], changes in bottom-water calcite saturation [14], and margin scavenging [15,16]. Due to the contradictory indications from different paleocirculation proxies, there is currently no consensus regarding the effects of climate on global ocean circulation.

Nd isotope ratios in the dispersed authigenic ferromanganese oxide precipitates in sediments have attributes that make them potentially useful as a paleocirculation proxy and which can break this deadlock. Here we present a detailed Nd isotope record of core RC11-83 (41.07°S, 9.717°E, 4718 m) from southeast Atlantic (Fig. 1) between ~20 and ~6 kyr cal. BP, covering the Last Glacial Maximum (LGM) to the early middle Holocene. The core is from a drift deposit in the southern Cape Basin and accumulates with an average sedimentation rate of ~20 cm/kyr [6]. We also report new Holocene and LGM samples from core TNO57-6 (42.92°S, 8.88°E, 3750 m), from the south side of the Agulhas Ridge and thus outside of the Cape Basin. Two previous studies concluded that the Nd isotope variability on longer time scales in Cape Basin cores records waxing and waning of NADW export to the Southern Ocean during warm and cold climate stages through the last glacial cycle [17,18]. The new RC11-83 record presented here has an average sample spacing of 300 years (43 samples over ~14 kyr) and thus can test the relationship between NADW strength and rapid climate change through the Termination interval. The new data indicate a baseline increase in NADW intensity beginning approximately between 18 and

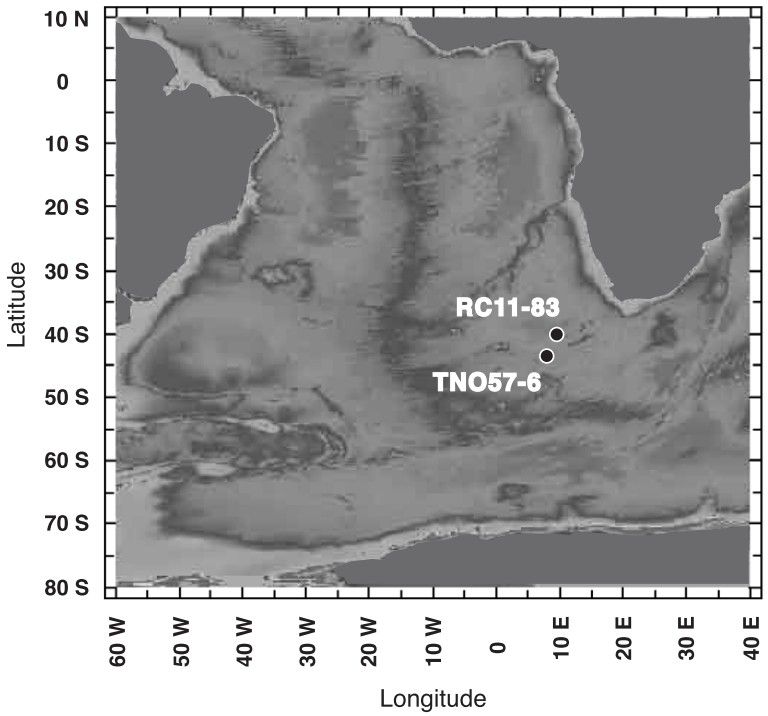

Fig. 1. Map of the South Atlantic Ocean showing the sites of cores RC11-83 and TN057-6.

17 kyr that parallels increasing Northern Hemisphere insolation and atmospheric CO_2 abundance. This baseline increase is overprinted by millennial increases in NADW intensity associated with Northern Hemisphere abrupt warmings and changes in sea ice cover. Prior to the Bølling warming, the record of NADW strength shows a series of variations, which correlate to well-dated climate excursions in Europe and changes in North Atlantic sea ice extent. The amount of NADW reaching the Cape Basin strengthened during the Bølling warming, weakened during the Allerød cooling, reached a minimum at the start of the Younger Dryas event, and thenceforth strengthened to reach Holocene values. The data show that Nd isotopes can be a sensitive monitor of short- and long-term changes in the global overturning circulation.

2. Nd isotope ratios as a paleocirculation proxy

The potential for using Nd isotope ratios as a paleocirculation proxy stems from its systematic geographic variability in the oceans. In bottom-water and Fe–Mn nodule and crust surfaces, Nd isotope ratios are geographically distinct and vary over a large range from low values of $\varepsilon_{Nd} < -20$ in the Labrador Sea, to values as high as $\varepsilon_{Nd} \sim 0$ in the Pacific [19–25]. Water column profiles show that water masses conserve the Nd isotopic fingerprints of their source regions over long transport paths. For example, the NADW Nd isotope signature ($\varepsilon_{Nd} \sim -14$) can be traced southward into the South Atlantic, and the Antarctic Bottom Water (AABW) signature ($\varepsilon_{Nd} \sim -7$ to -9) can be traced northward [26].

Nd isotopes do not share the same sources of uncertainty as conventional nutrient and U-series paleocirculation proxies and thus can complement them. The high atomic masses of the isotopes of Nd (142–150 AMU) combined with a single oxidation state (+3) inhibits significant mass fractionation by biological and other low-temperature processes, in contrast to low mass-stable isotope proxies. Moreover, any natural mass-dependent fractionation is accounted for by corrections applied during measurement by mass spectrometry. Thus, the variability of $^{143}Nd/^{144}Nd$ ratios reflects the long-lived radioactive decay of ^{147}Sm to ^{143}Nd (half-life = 106 Ga), and the measured Nd isotope ratio in an authigenic phase directly reflects the seawater source as long as there has been no later addition of Nd through diagenesis. Along the transport path of a water mass the Nd isotope ratio is conserved even if the concentration is not, and variability reflects either mixing of water masses or addition of a new component of Nd. Authigenic Fe–Mn oxides have high concentrations of Nd, and the Nd isotope ratios reflect the seawater sources from which they precipitate. For this reason, there has been a significant focus on Fe–Mn crusts to temporally trace ocean circulation (cf. [24,25], and references therein). For example, Frank [24] concluded that the average global overturning circulation intensity declined due to growth of the Northern Hemisphere ice sheets, based on data from Southern Ocean Fe–Mn crusts. However, the slow growth rates of the Fe–Mn crusts (10^5–10^6 year per mm) limit the applicability of Nd isotopes to address short timescale changes in ocean circulation. Because each measured sample integrates over several glacial cycles, the signal does not distinguish between a general decline and the effects of a weaker "conveyor" during glacial periods. Palmer and Elderfield [27] published the first down-core record of Nd isotope ratios of Fe–Mn encrusted foraminifera, addressing changes in South Atlantic seawater over tens of millions of years. Recent studies have demonstrated Nd isotopic variability in the oceans on glacial–interglacial timescales by measuring the leachable Fe–Mn oxide components of deep-sea cores [17,18] and foraminiferal $CaCO_3$ [28].

Rutberg et al. [17] showed that Nd isotope ratios in the authigenic Fe–Mn component vary systematically through the last ice age in RC11-83, with lower values during marine isotope stages (MIS) 1 and 3 and higher values during MIS 2 and 4, consistent with waxing and waning of NADW intensity during warm and cold climate periods, respectively. During MIS 2 and 4, Nd isotope ratios were higher than present day AABW, indicating a stronger Pacific component in the Circum-Antarctic during cold climate stages. The Nd isotope variations in RC11-83 generally follow benthic foraminiferal $\delta^{13}C$ variations, previously interpreted to reflect changes in the NADW export to the Southern Ocean [6,29]. Rutberg et al. [17] also showed the same sense of change in TNO57-6 from

the Holocene to the LGM. Subsequently, Bayon et al. [18] reported a record on a core from the northern Cape Basin (MD96-2086, 25.81°S, 12.13°E, 3606 mbsl), which shows a similar Holocene–LGM pattern, with more NADW-like Nd isotopes during the Holocene and nearly the same Nd isotope ratios as RC11-83 during the LGM.

Rutberg et al. [17] evaluated the integrity of the marine signal in RC11-83 in two ways. Sr isotope ratios of the Fe–Mn oxide leachates were found to be the same as Pleistocene–Holocene seawater (~ 0.7092) and were much lower than associated terrigenous detritus (0.717–0.723), thus showing that there is no detrital contamination of the Sr. In addition, they used the present-day hydrography. The bottom water currently in contact with RC11-83 is a $\sim$ 30:70 NADW–AABW mixture ($SiO_2 \sim 100$ pmol/kg, salinity ~ 34.7 psu, $T \sim 1$°C) [30]. The nearest literature seawater Nd isotope profile is from the southern Angola Basin, north of the Walvis Ridge at 30°S, 1.42°W, and shows a zigzag pattern reflecting Antarctic Intermediate Water (AAIW) at intermediate depths and a mixture of NADW–AABW at deeper depths [26]. Nd isotope ratios in deep Atlantic seawater correlate with indicators of the mixing proportions of NADW–AABW such as salinity and SiO_2 (reviewed in [25]). Rutberg et al. [17] show that the Nd isotope ratio of their youngest Fe–Mn oxide leachate, plotted with the average annual dissolved SiO_2 of the bottom water, falls on the present-day Atlantic seawater SiO_2–ε_{Nd} correlation, indicating that the Nd is derived from the deep water. Bayon et al. [18] show that the youngest sample of MD96-2086 falls on the same correlation, despite slightly high Sr isotope ratios of ~ 0.7093, and conclude that the leachate Nd isotope ratios reflect the deep seawater despite slight contamination of the leachate Sr by detritus. The lower (more NADW-like) Nd isotope ratios in the MD96-2086 sample, compared with RC11-83, thus appears to reflect the stronger NADW signature of the ambient seawater at its location. In addition, Bayon et al. [18] show that the rare earth element patterns of the leachates match the distinctive pattern of seawater. These data, together with the observation that the Nd isotope ratios of the LGM samples of both cores yield the same values, strongly indicate that the Nd isotope ratios of the Fe–Mn oxide leachates in these cores preserve the signal of the deepwater masses.

3. Analytical procedures and results

Bulk samples from RC11-83 (typically ~ 0.7 g) were treated with buffered acetic acid to remove carbonate, then leached with 0.02 M hydroxylamine hydrochloride (HH) to dissolve Fe–Mn oxyhydroxides. Nd and Sr were separated from the leachate using Eichrom Sr-spec™ and Tru-spec™ resin [17]. Nd and Sr isotope ratios were measured at Lamont–Doherty Earth Observatory using a Micromass Sector 54-30 thermal ionization mass spectrometer. Nd and Sr isotope data are listed in Table 1 and analytical details are given in the caption.

In order to better constrain the down-core ages of RC11-83 during the Termination interval, we have extended the ^{14}C chronology [6,29] with six additional dates on planktonic foraminifera (Table 2). The new ages are consistent with previous studies and further refine the down-core chronology. The ^{14}C ages are converted to calendar years using INTCAL [31] to 15.5 kyr cal. BP, where the spliced tree ring-based comparison ends. U–Th and ^{14}C ages of corals [32] are used from 15.5 to 21 kyr cal. BP. The down-core age model is optimized to smooth abrupt apparent changes in the sedimentation rate, keeping individual ^{14}C ages within the range allowed by the ^{14}C age errors and the INTCAL calibration (Table 2). Ages between ^{14}C ages, listed in Table 1, are linearly interpolated.

The new RC11-83 Nd isotope data (Fig. 2) show a general decrease from LGM depths ($\varepsilon_{Nd} \approx -6.5$) at ~ 400 cm, reaching Holocene values at ~ 160 cm ($\varepsilon_{Nd} \approx -9.4$). Superimposed on this baseline decline are several millennial excursions. New Holocene and LGM samples from TNO57-6 were analyzed as a crosscheck on two samples reported by Rutberg et al. [17]. They are from similar but slightly different depths in the core (21 and 70 cm vs. 15 and 60 cm) and confirm a decrease in the Nd isotope ratios from the LGM to the Holocene. The integrity of the down-core seawater signal in the Fe–Mn leachates was checked by Sr isotopes measurements on nearly all samples (Table 1). In all cases, they were found to be marine ($^{87}Sr/^{86}Sr = 0.709176 \pm 0.000028$ 2σ, for the entire data set). The entire deviation is similar to the estimated reproducibility (± 0.000023 2σ, Table 1); thus, all the data are effectively within error. Sr isotope ratios of the terrigenous detritus component

Table 1
Nd and Sr isotope ratios of RC11-83 Fe–Mn–oxide leachates

Depth in core (cm)	Age (kyr-cal. BP)	$^{143}Nd/^{144}Nd$	ε_{Nd}	$^{87}Sr/^{86}Sr$
84	6.30	0.512159 ± 08	−9.34 ± 0.16	0.709164 ± 16
100	6.98	0.512161 ± 09	−9.31 ± 0.18	0.709214 ± 50
117	7.71	0.512167 ± 08	−9.18 ± 0.16	0.709165 ± 18
125	8.06	0.512180 ± 07	−8.93 ± 0.14	
126	8.10	0.512204 ± 08	−8.46 ± 0.16	0.709167 ± 11
132	8.28	0.512162 ± 08	−9.28 ± 0.16	0.709143 ± 16
164	9.27	0.512145 ± 06	−9.61 ± 0.11	
165	9.32	0.512176 ± 07	−9.02 ± 0.14	
169	9.51	0.512203 ± 08	−8.49 ± 0.16	0.709217 ± 13
174	9.74	0.512177 ± 09	−8.99 ± 0.18	
180	10.02	0.512159 ± 06	−9.34 ± 0.12	0.709172 ± 20
191	10.54	0.512198 ± 07	−8.58 ± 0.14	0.709189 ± 14
201	11.01	0.512204 ± 08	−8.46 ± 0.16	0.709220 ± 09
205	11.20	0.512216 ± 08	−8.22 ± 0.16	0.709161 ± 20
209	11.75	0.512223 ± 07	−8.09 ± 0.14	0.709217 ± 17
211	12.03	0.512224 ± 09	−8.08 ± 0.18	0.709186 ± 10
213	12.30	0.512240 ± 07	−7.76 ± 0.14	0.709192 ± 10
217	12.85	0.512269 ± 04	−7.18 ± 0.08	0.709169 ± 18
221	13.40	0.512253 ± 07	−7.52 ± 0.13	0.709227 ± 11
225	13.55	0.512226 ± 08	−8.04 ± 0.16	0.709161 ± 14
230	13.74	0.512240 ± 08	−7.75 ± 0.16	0.709169 ± 18
235	13.96	0.512226 ± 08	−8.04 ± 0.16	0.709200 ± 13
244	14.37	0.512186 ± 06	−8.82 ± 0.11	0.709194 ± 14
249	14.54	0.512249 ± 06	−7.59 ± 0.12	0.709175 ± 48
250	14.57	0.512261 ± 12	−7.35 ± 0.24	0.709170 ± 17
259	14.87	0.512184 ± 09	−8.85 ± 0.18	
260	14.89	0.512212 ± 06	−8.30 ± 0.13	0.709140 ± 17
262	14.96	0.512271 ± 08	−7.15 ± 0.16	0.709163 ± 11
263	14.99	0.512262 ± 09	−7.32 ± 0.18	0.709159 ± 14
267	15.15	0.512269 ± 06	−7.21 ± 0.11	0.709120 ± 11
268	15.18	0.512274 ± 07	−7.11 ± 0.14	0.709161 ± 11
270	15.26	0.512314 ± 15	−6.32 ± 0.30	
273	15.37	0.512331 ± 06	−5.99 ± 0.12	
275	15.44	0.512237 ± 05	−7.83 ± 0.10	0.709177 ± 13
277	15.52	0.512223 ± 08	−8.09 ± 0.16	0.709177 ± 27
280	15.63	0.512281 ± 09	−6.96 ± 0.18	0.709147 ± 06
284	15.78	0.512261 ± 06	−7.36 ± 0.12	0.709179 ± 13
285	15.82	0.512274 ± 07	−7.11 ± 0.14	
301	16.43	0.512281 ± 07	−6.96 ± 0.14	0.709164 ± 13
308	16.75	0.512262 ± 08	−7.33 ± 0.16	
315	17.06	0.512260 ± 07	−7.37 ± 0.16	
335	17.96	0.512304 ± 06	−6.52 ± 0.14	0.709142 ± 23
355	18.49	0.512303 ± 07	−6.53 ± 0.16	
398	20.36	0.512310 ± 08	−6.40 ± 0.22	
TNO57-6				
21	Holocene	0.512279 ± 11	−7.69 ± 0.21	0.709218 ± 11
70	LGM	0.512389 ± 11	−5.55 ± 0.21	0.709190 ± 11

Table 2
New RC11-83 radiocarbon ages

Depth in core (cm)	Sample type	^{14}C age (kyr BP)	Calendar age (kyr BP)
112	inflata	5.26 ± 0.05	6.10
163	mixed	8.15 ± 0.04	9.00
163	inflata	8.29 ± 0.06	
205	mixed	9.76 ± 0.04	11.21
205	inflata	9.80 ± 0.06	
277	mixed	12.40 ± 0.07	15.60
277	inflata	12.80 ± 0.09	
368	mixed	16.15 ± 0.09	19.00
390	mixed	16.65 ± 0.11	19.70

The new ages augment those previously published in [6,29] and are Libby ages. Measurements were made at NOSAMS–WHOI except the samples at 163 and 205 cm which were made at Lawrence Livermore National Laboratory. Reported errors are 1σ. A reservoir correction of 600 years has been applied, as in the previous studies. Conversion to calendar ages used the INTCAL [31] and coral [32] curves as explained in the text.

of the same samples are much higher throughout RC11-83, ranging from 0.717 to 0.723 [33]. The results indicate negligible exchange between the Fe–Mn oxides and associated terrigenous detritus because with such a large difference in $^{87}Sr/^{86}Sr$ ratios, even a small amount of detrital Sr would be easily detected. For example, if the difference between the highest measured leachate value (0.709227) and the average (0.709176) were assumed to be due to contamination by detritus with $^{87}Sr/^{86}Sr \sim 0.717$, it would reflect a negligible contamination level of 6‰ As Sr is much more soluble than Nd, it can be

Notes to Table 1:
Sr and Nd isotope ratios were measured at Lamont–Doherty Earth Observatory on a Micromass Sector 54-30 thermal ionization mass spectrometer by dynamic multicollection. $^{87}Sr/^{86}Sr$ ratios were normalized to $^{86}Sr/^{88}Sr = 0.1194$, with typical ^{88}Sr beam intensities of $3–5 \times 10^{-11}$ A. Replications of the NBS987 standard yielded 0.710269 (± 0.000023, 2σ external reproducibility, $n = 56$), and all samples were corrected to a value of 0.710230. Most of the Sr isotope ratios are based on between 50 and 100 measurements, fewer than for most studies in the same lab, because the primary objective was to determine if the $^{87}Sr/^{86}Sr$ ratio is marine, rather than to measure to high precision. $^{143}Nd/^{144}Nd$ ratios were measured as NdO^+ and normalized to $^{146}Nd/^{144}Nd = 0.7219$, with typical ^{144}Nd beam intensities of 0.5×10^{-11} A. Replications of the La Jolla Nd standard averaged 0.511832 (± 0.000016, 2σ external reproducibility, $n = 164$), and $^{143}Nd/^{144}Nd$ ratios are corrected to a value of 0.511860. Nd isotope ratios are presented as ε_{Nd}, the deviation from the chondritic value of $^{143}Nd/^{144}Nd = 0.512638$ in parts per 10,000 [71]. Errors listed are internal measurement errors.

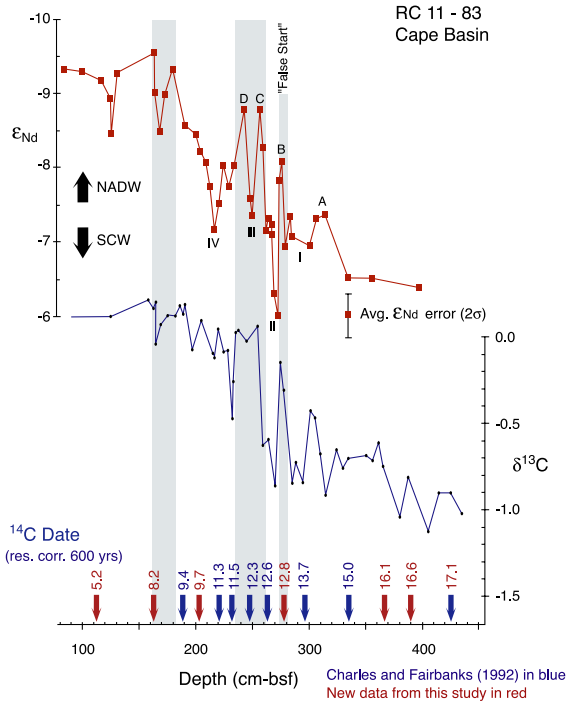

Fig. 2. $\delta^{13}C$ of benthic foraminfera, Nd isotope ratios of the authigenic Fe–Mn oxide component and ^{14}C ages vs. depth for RC11-83. Nd isotope ratios are plotted as ε_{Nd} and are on a reverse axis for comparison purposes. Error bars are the 2σ external reproducibility of the La Jolla Nd standard, reflecting the best error estimate for samples measured once. All of the samples associated with peaks and troughs were measured at least twice.

expected that the level of any contamination by detrital Nd is lower. As noted above, a core from the northern Cape Basin shows no indication of detrital contamination of the Nd in Fe–Mn oxide leachates despite a Sr isotope ratio slightly higher than seawater [18].

4. Benthic foraminiferal $\delta^{13}C$ and Nd isotope profiles of RC11-83

The patterns of Nd isotope and benthic foraminiferal $\delta^{13}C$ variability display a high degree of coherency (Fig. 2). Despite different geochemical cycling of Nd and carbon in the oceans, both the ε_{Nd} and benthic foraminiferal $\delta^{13}C$ records of RC11-83 exhibit a similar glacial-to-Holocene trend. Moreover, much of the millennial-scale detail can be directly correlated, including the "false start" of NADW production suggested by Charles and Fairbanks [6] prior to the Bølling warming (275 cm bsf., 12.8 ^{14}C kyr BP). To the extent that the shifts in the Nd isotope ratios reflect changes in the mixture of NADW and AABW overlying RC11-83, produced by strengthening and weakening of the global overturning circulation, the coherency with the benthic foraminiferal $\delta^{13}C$ indicates that its pattern also primarily reflects these changes, with the low glacial $\delta^{13}C$ values possibly amplified by productivity changes (cf. [6,12,29]).

As this study presents the first Nd isotope record of deep ocean circulation at submillennial time resolution, the inferred changes in NADW export need to be confirmed at other core sites. In this context, we note that agreement with the results of Bayon et al. [18] from the northern Cape Basin at lower time resolution lend credence to the validity of Nd isotopes as a paleocirculation tracer.

The validity of our interpretation of the Nd isotope pattern as reflecting changes in the global overturning circulation intensity depends on the assumption that the variability does not simply reflect shifts in Nd isotope ratios or Nd concentrations of the end-member water masses or along the transport path. Processes that could affect the Nd isotope ratio of South Atlantic deep waters include additional sources of Nd to the South Atlantic, a variable residence time of deep Atlantic Nd through time, or changes in the Nd isotope ratio or concentration in the NADW or Pacific end-members. An extensive discussion of these effects, and the reasons why the variability appears to reflect changes in ocean circulation, is given in Rutberg et al. [17]. We summarize the current constraints on the end-member isotope ratios here. The constancy of the Pacific end-member over glacial–interglacial cycles is evidenced by constancy of Nd isotope ratios ($\varepsilon_{Nd} \sim -4$) of a Fe–Mn crust sampled at a time resolution of a few thousand years through MIS 1–6 [34] and constancy in manganiferous sediments from near the East Pacific Rise [35]. Constraining the Nd isotope ratio of the North Atlantic end-member through time is more problematic due to encroachment of AABW into the North Atlantic during cold intervals, and this might be addressed in future studies by measuring downcore records of several cores from different water depths, or a site which was always bathed in pure NADW. Rutberg

et al. ([17], in their Fig. 2a) evaluated the North Atlantic end-member indirectly based on data from the surfaces of Mn nodules and crusts. These samples generally represent averages over 10^5–10^6 years, encompassing several glacial cycles. South Atlantic Nd isotope ratios, plotted against SiO_2 of bottom waters, are offset to high ε_{Nd} compared to the modern seawater dissolved SiO_2–ε_{Nd} trend, consistent with relative weakening of NADW and strengthening of the Pacific signal during cold climate stages. In contrast, virtually all of the Pacific data lie on the modern dissolved SiO_2–ε_{Nd} trend, consistent with the independent data summarized above indicating broad constancy of Nd isotope ratios through glacial cycles. Most of the North Atlantic data also lie on the modern dissolved SiO_2–ε_{Nd} trend, which we interpret to indicate a roughly constant NADW Nd isotopic signature. A few North Atlantic Fe–Mn crust samples lie at higher ε_{Nd} (like most South Atlantic samples), probably reflecting glacial encroachment of AABW into the North Atlantic. Only one has lower ε_{Nd} than predicted by the dissolved SiO_2 of bottom water.

The available Fe–Mn crust data thus indicate stable North Atlantic and Pacific end-members through the late Pleistocene. Throughout the following discussion, we assume that the temporal variations we observe in the South Atlantic primarily reflect changes in the proportions of the NADW and Pacific end-member water masses reaching the core site.

5. Comparison to Northern Hemisphere climate records

The improved ^{14}C chronology for RC11-83 allows us to address the link between deep-ocean circulation and climate by comparing the Nd isotope record, taken here as reflecting NADW intensity, with climate proxy records (Fig. 3). There appears to be a progressive baseline intensification of NADW through the deglaciation (18–14 kyr cal. BP), resembling the trend of increasing summer insolation at 65°N [36] and atmospheric CO_2 concentration [37]. Superimposed on the general increase of the NADW signal are significant millennial-scale fluctuations that appear to be reflected in some Northern Hemisphere climate records.

Greenland ice core $\delta^{18}O$, interpreted as reflecting paleotemperature, shows broad agreement with our Nd isotope record. The RC11-83 record indicates a strong peak in NADW intensity at the Bølling warming (peak D, Fig. 3), where the Nd isotope ratio reaches ~75% of its Holocene level compared to the LGM baseline. Conversely, the Allerød cooling is linked to a weakening of thermohaline circulation, where, at its minimum (trough IV, Fig. 3), the signal

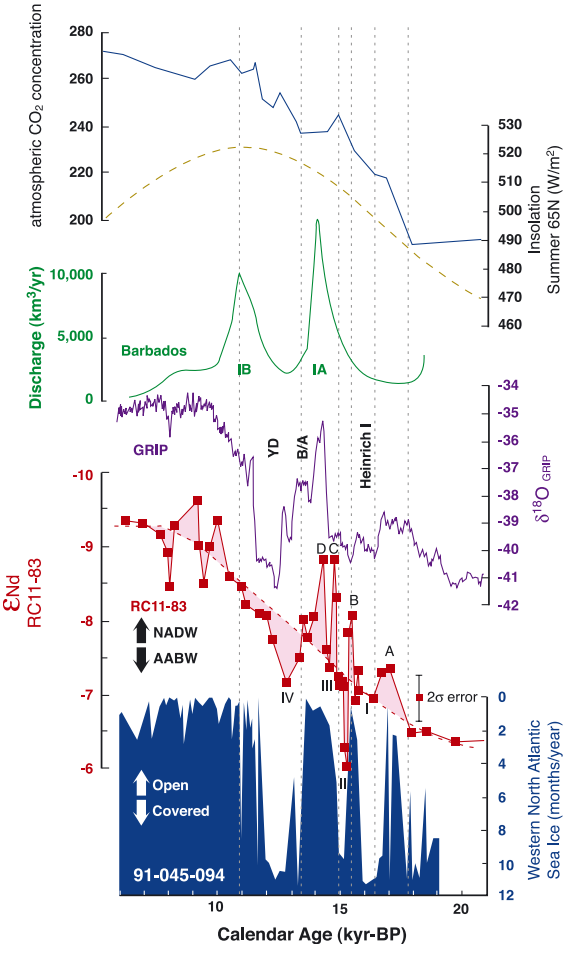

Fig. 3. Nd isotope ratios of RC11-83 and other climate records. Nd isotope ratios, reflecting NADW strength at the RC11-83 site, are plotted as ε_{Nd} and are on a reverse axis for comparison purposes. The sea ice record of core HU91-045-094 from the southern Labrador Sea (50°12.26′ N, 45°41.14′ W; 3448 mbsl) is from [38,39]. The Northern Hemisphere insolation curve is from [36], while the deglacial atmospheric CO_2 record is from [37]. The GRIP record is from [72,73].

is only ~25% higher than the LGM baseline. In detail, there are differences between these two records. For example, the progressive baseline increase in NADW intensity is not reflected in Greenland paleotemperature. Some of the pre-Bølling millennial-scale fluctuations in RC11-83 are not easily recognized in Greenland but are more similar to a high-resolution record of North Atlantic sea ice coverage [38,39] (Fig. 3).

6. Pre-Bølling NADW intensification

From high LGM values, Nd isotope ratios significantly decrease by 17.1 kyr cal. BP (peak A, Fig. 3), indicating increasing NADW flux to the South Atlantic, followed by a reversal that does not decrease to LGM values. The NADW signal shows substantial instability during the early part of the Termination period between 18 kyr cal. BP and the Bølling maximum warming at 14.3 kyr cal. BP, displaying three peaks (B, C, D in Fig. 3) and a prominent minimum (trough II, Fig. 3). These Nd isotopic variations are corroborated by multiple data within short depth intervals in RC11-83 (Table 1).

Although the Greenland ice record does not show the same variability during the pre-Bølling interval, there is substantial evidence for warming during this "Oldest Dryas" period in North Atlantic continental and marine climate records (e.g., [40], and references therein). Increases in juniper, birch, and pine pollen concentrations document a shift from pleniglacial conditions to warmer climate in Europe at ~17 kyr cal. BP, corresponding to the first stepwise increase of the NADW signal (peak A, Fig. 3). The period between 15.5 and 14.5 kyr ^{14}C BP (18.5–17.0 kyr cal. BP) saw deglaciation in the Alps, retreat of the Baltic ice sheets [40], and reduced sea ice in the Norwegian Sea [41] and western North Atlantic [38,39]. Surface water temperatures in the Norwegian Sea increased between 13.4 and 13.1 kyr ^{14}C BP (15.7–16.3 kyr cal. BP), reaching near modern values [41], concurrent with the sharp increase in the NADW signal at 15.6 kyr cal. BP (peak B, Fig. 3). The absence of comparable pre-Bølling temperature excursions in the ice core record suggests that Greenland may have been isolated from other climate changes in the North Atlantic and Europe [42]. Alternatively, the δ^{18}O of precipitation may have been affected by processes other than local temperature such as changes in the moisture source or distillation path length [6,43]. Although the Greenland δ^{18}O records exhibit muted changes during the early deglaciation, it appears that unstable, short-term NADW increases accompanied pre-Bølling climate amelioration in Europe.

The Nd isotope data also indicate major short-term waxing and waning of the NADW signal prior to the Bølling warming, with the peak B event rapidly followed by a major weakening during the trough II event (Fig. 3). The peak was recognized by Charles and Fairbanks [6] in the benthic foraminiferal δ^{13}C data and attributed to a "false start" of NADW production. The timing of this event also coincides with a sudden change in the ventilation rate of the North Atlantic, as recorded by the ^{14}C ages of deep-sea corals [44]. The U–Th ages of these corals are 15.41 ± 0.17 kyr. Their ^{14}C ages increased by as much as 670 years during their life span and are accompanied by a change in Cd/Ca, reflecting increased nutrient content. Age uncertainties allow for either or both of these Nd isotopic excursions in RC11-83 to be a reaction to Heinrich event 1 (H1), which is generally correlated with the δ^{18}O minimum in the Greenland ice record prior to the Bølling warming [45]. As the Nd isotope ratio of trough II (Fig. 3) is more Pacific-like than the LGM value, this may reflect a major, short-term (~500 year) weakening of NADW in response to H1. This is consistent with the ^{231}Pa/^{230}Th record from Bermuda Rise core OCE326-GGC5, which indicates an NADW shutdown during H1 [46], as well as deep-sea coral Cd/Ca data [44], indicating southern source water at intermediate depths in the North Atlantic.

Ruddiman and Mcintyre [47] showed that sea ice in the North Atlantic retreated during the deglaciation from southern maxima during the LGM and Younger Dryas to more ice-free conditions during the Bølling warming and the Holocene. A high-resolution record of sea ice cover from dinoflagellate cyst assemblages in core HU91-045-094, from the northwest North Atlantic (50°12.26′ N, 45°41.14′ W, depth 3448 m) [38,39] shows a strong correspondence to our Nd isotope record (Fig. 3). During the pre-Bølling interval, when the NADW signal is highly variable, there is a remarkable correlation between NADW intensity

peaks (shaded areas above the dashed line in Fig. 3) and sea ice reductions. These include peaks A, B, C (~ 17, 15.6, 14.9 kyr cal. BP, respectively). During the Bølling warming, when sea ice cover was limited to a few months per year, we observe a strong NADW signal (peak D). In addition, weakening of NADW to or below baseline levels (shaded areas below the dashed line in Fig. 3) correspond to increased sea ice coverage. The most extreme reduction in NADW strength during the deglaciation (trough II, Fig. 3) corresponds to a period of high sea ice coverage prior to the Bølling warming. During the Allerød and Younger Dryas, a long interval of sea ice cover also accompanies an NADW minimum. Altogether, the comparison strongly indicates that open water conditions at 50°N were concurrent with periods of increased presence of NADW in the Southern Ocean, and vice versa.

7. Mechanisms for millennial fluctuations

Previous studies in the North Atlantic using benthic foraminiferal $\delta^{13}C$ have concluded that the global overturning circulation was variable during the last ice age (MIS 2–4) and was subject to abrupt changes during Dansgaard–Oeschger abrupt warmings and/or Heinrich events [48]. As these proxies can be affected by biological effects, the Nd isotope record for RC11-83 provides an independent confirmation for millennial abrupt changes in deep ocean circulation. Here we discuss some possible causes.

Can the RC11-83 record be corroborated with records of freshwater input to the North Atlantic? Relationships to major Northern Hemisphere ice sheet melting events are not evident (Fig. 3). For example, at most only a small negative perturbation of the NADW signal is seen during meltwater pulse (MWP) IB just prior to the onset of the Holocene, which is followed by a sharp increase in NADW intensity. The NADW signal reached near Holocene levels around the time of MWP IA during the Bølling warming, although a relationship between MWP IA and the post-Bølling weakening cannot be ruled out. It is possible that the thermohaline response to MWP IA appears as trough III, a short-lived decrease in NADW strength. Based on our chronology, the beginning of the Bølling and MWP IA are concurrent with peak D, and trough III would precede both climate events. We cannot completely rule out errors in the age modeling of ice cores, or changes in the ^{14}C reservoir age correction used for our ages, which together might allow the true ages of trough III and MWP IA to be within error (although we observe no sudden shifts in sedimentation rate for RC11-83, which should be accompanied by an incorrect age model). If they are related, then the data show that the North Atlantic response to rapid meltwater discharge was short-lived because NADW returned to its previous strength within a few hundred years of the event. It is also possible that a real reduction in circulation strength during the Bølling and MWP IA was masked by a change in the Nd isotope signature of NADW. We consider this to be unlikely because the benthic carbon isotopes also indicate stronger NADW during this time period.

The Nd isotope data are consistent with the observation by Fairbanks [49] that the major meltwater events are not associated with Northern Hemisphere cooling caused by NADW cessation over millennial timescales. Coupled ocean–atmosphere models have also suggested a slow and lagged response of NADW to meltwater events. Rind et al. [50] reported that the addition of the estimated flux of MWP IA (0.15 Sv over 1.56 kyr) to the GISS coupled ocean–atmosphere GCM produced only a small reduction in NADW formation. Manabe and Stouffer [51] modelled the response of deepwater formation to freshwater input and found that a massive meltwater pulse would cause an abrupt weakening of NADW, followed by a series of oscillatory strengthening and weakening of deepwater formation. Our Nd isotope record of NADW history during parts of the deglaciation is more similar to this modelled response than it is to models which generate a prolonged shutdown. The structure of NADW variations in response to meltwater pulses lends empirical credence to the idea that the effects of the meltwater pulses on the NADW flux are extremely short-lived.

The correlation between NADW intensity peaks and sea ice reductions in the North Atlantic (Fig. 3) suggest that sea ice coverage in the North Atlantic is correlated to the millennial-scale changes in NADW production during the deglaciation because it physically constrained the latitude of advection in the North Atlantic. Rapid changes in sea ice coverage, especial-

ly in the Labrador Sea, are a possible mechanism to rapidly shift circum-North Atlantic climate between maritime and continental conditions [52,53]. The southern-most limit of sea ice extent in the North Atlantic is controlled by the position of the polar front boundary which is ultimately controlled by atmospheric circulation [54]. Sea ice export from the Arctic Ocean appears to be mainly controlled by atmospheric and sea surface dynamics [55–57] related to North Atlantic Oscillation (NAO) cycles [58]. Observations of the modern North Atlantic show that deepwater formation is also linked to NAO cycles. For example, the strength of Denmark Strait overflow waters follow NAO-induced changes in the hydrographic properties of the Fram Strait [59]. As deepwater formation and sea ice extent covary with atmospheric-forced NAO cycles today, the observation that these two variables covaried in the paleorecord suggests an atmospheric forcing for rapid climate and thermohaline circulation changes in the past.

Alternatively, changes in thermohaline circulation might be expected to modulate northward heat transport, thereby affecting sea ice conditions. However, Seager et al. [60] determined that modern-day pole-ward ocean heat transport becomes progressively less important compared to seasonal ocean heat storage and release of solar radiation at latitudes south of 60°N in the North Atlantic. This suggests that changes in pole-ward ocean heat transport were not the primary control on the latitude of the sea ice edge when it was located further south during the deglacial. In addition, simple ocean models and three-dimensional general circulation models have been thus far unable to reproduce the rapid shifts recorded in climate records by abruptly changing NADW production [61,62]. For example, when NADW production is reduced, the climate responses in the models are muted, lagging the cessation and recovery of NADW production by hundreds of years. To the extent that these results reflect the real climate system, they suggest that oscillations in thermohaline circulation strength may not be the primary reason for abrupt changes to North Atlantic temperature, and by extension, sea ice extent.

The records of sea ice coverage document great variability during the early deglaciation compared to the early Holocene. Our record suggests that early in the deglaciation, short-lived fluctuations in NADW formation occurred, while during the later deglaciation, ocean circulation changes became more gradual. If the location of the southern limit of North Atlantic sea ice cover controls NADW production, the high variability in NADW strength during the deglaciation may reflect the increased importance of wind-driven sea ice export, rather than insolation-driven sea ice production.

8. Progressive NADW intensification during the deglaciation

The RC11-83 Nd isotope record allows new insights into the factors that influence glacial–interglacial changes in NADW production. The progressive baseline increase in NADW (dashed line in Fig. 3) appears as a real characteristic of this record. It is not an ‘‘averaging’’ effect due to bioturbation or remobilization of Fe–Mn oxides, because the gradual deglacial trend is observed over ~150 cm of core length, and contains fluctuations on short length scales. If bioturbation had produced the gradual trend in Nd isotopes during the deglaciation, it would have the observed millennial excursions over length scales of tens of centimeters. In addition, this same pattern is apparent in much of the benthic foraminiferal $\delta^{13}C$ record ([6] and Fig. 2).

We propose that increasing insolation throughout the deglaciation allowed stronger potential deepwater production, and this occurred when sea ice-free conditions in the North Atlantic promoted surface convection. The successive increases in the maximum NADW signal shown by peaks A, B, C (Fig. 3) suggest a greater capacity to produce NADW as deglaciation progressed. Most of the early deglacial events (peaks A, B, C, D, and trough II), which we correlate to changes in sea ice coverage, were clearly not shifts to a Holocene equilibrium state, as each are followed by a return to a ‘‘baseline’’ level of NADW strength. Moreover, while we observe a substantial weakening during the Allerød, it does not represent a full return to ‘‘glacial mode’’ conditions. We also interpret our record to show that NADW was systematically intensifying during much of the Younger Dryas, from a minimum (trough IV) at the Allerød–Younger Dryas boundary.

A gradually changing baseline record of deepwater production is not easy to reconcile with paleocirculation and paleoclimate records that appear to indicate rapid switches between distinct "modes" of deepwater production. The negative buoyancy of North Atlantic surface waters is driven by salinity; therefore, increased freshwater flux from melting of continental glaciers is expected to cause weakening of NADW intensity [2]. If fresh water input to the North Atlantic is low, downwelling occurs at high latitudes and thermohaline circulation is robust. Higher fresh-water input poisons the northern mode, and a weaker southern mode ensues with downwelling at temperate latitudes [63]. Some ocean circulation models have emphasized the sensitivity of NADW formation to sudden increases in fresh water into the North Atlantic. Many ocean and climate proxies saturate at high and low values (e.g., abundance of pachyderma left), which may lead to the impression of a rapid switch from one state to another. In contrast to these proxies, the Nd isotope signal is continuous, reflecting the extent of mixing between northern-and southern-sourced waters at the core site. Although the peaks and troughs in Fig. 3 indicate rapid changes between weak and strong thermohaline circulation, the progressively increasing baseline NADW intensity indicates a continuum between the "Holocene" and "Glacial" modes of circulation. As previously noted, during the Younger Dryas the NADW signal in the Cape Basin was intermediate between glacial and Holocene values, not a return to glacial conditions. The gradual increase in deepwater production is likely a response to deepwater formation at progressively higher latitudes, forced by increasing Northern Hemisphere insolation and perhaps magnified by increasing atmospheric CO_2 concentration.

9. A first attempt to quantify deepwater circulation changes

For reasons previously outlined, we consider the pattern of Nd isotope variability in RC11-83 to reflect the changes in NADW export to the Southern Ocean through the deglaciation. Unlike nutrient elemental and stable isotope tracers of ocean circulation, which are locally affected by productivity, air-sea gas exchange, and dissolution, Nd isotope ratios provide the potential to quantify ocean circulation changes. In this context, we have made a first attempt to use the data to estimate relative changes in the mixing proportions between NADW and Pacific end-members at the core site (Fig. 4). The estimate assumes that deepwater formation occurred primarily in the North Atlantic and that the Nd isotopes primarily reflect contributions of Nd ultimately from the North Atlantic and the Pacific, as in the present day (cf. [25]). The estimate of the fractional change in NADW–Pacific mixing does not use the benthic foraminiferal $\delta^{13}C$ because of the nonconservative behavior of carbon in the ocean. The estimate requires simplifying assumptions that may change with further work, but we maintain they are reasonable based on currently available data.

Firstly, we use modern end-member Nd isotope ratios and concentrations for Atlantic and Pacific end-members ($\varepsilon_{Nd} = -14$, Nd = 17 pmol/kg for NADW; $\varepsilon_{Nd} = -4$, Nd = 40 pmol/kg for Pacific; cf. [25]) and assume they were stable between the LGM and early Holocene. It is possible that differences in glacial versus interglacial weathering affected the inputs of Nd to the oceans (e.g., [64]), especially in the North Atlantic. Recent studies of terrigenous detritus in the northwest Atlantic show that off southern Labrador, at Orphan Knoll ($\sim 51°N$), Nd isotope ratios decreased from typical values of $\varepsilon_{Nd} \sim -12$ to -16 during the Holocene to -17 to -20 during the LGM [65,66]. Over the same time frame near the Greenland Rise in the Labrador Sea ($\sim 58°N$), they increased from typical values of $\varepsilon_{Nd} \sim -22$ to ~ -19. In any case, changes in the Nd isotopic ratio of terrigenous detritus do not necessarily imply changes in the isotope ratio dissolved Nd. While it is still unclear how the Nd isotope ratios are imparted to deep water (cf. discussion in [25]), strong evidence exists that Nd isotope ratios of terrigenous detritus in the deep sea are not the controlling factor for Nd isotopes in deep seawater. Early comparisons of Mn nodules and associated terrigenous sediments demonstrated significant differences [21]. The clearest evidence against simple control of deepwater Nd by exchange with sediment is from the northwest Pacific where there is a significant influx of eolian dust from China and high Nd isotope ratios of deep

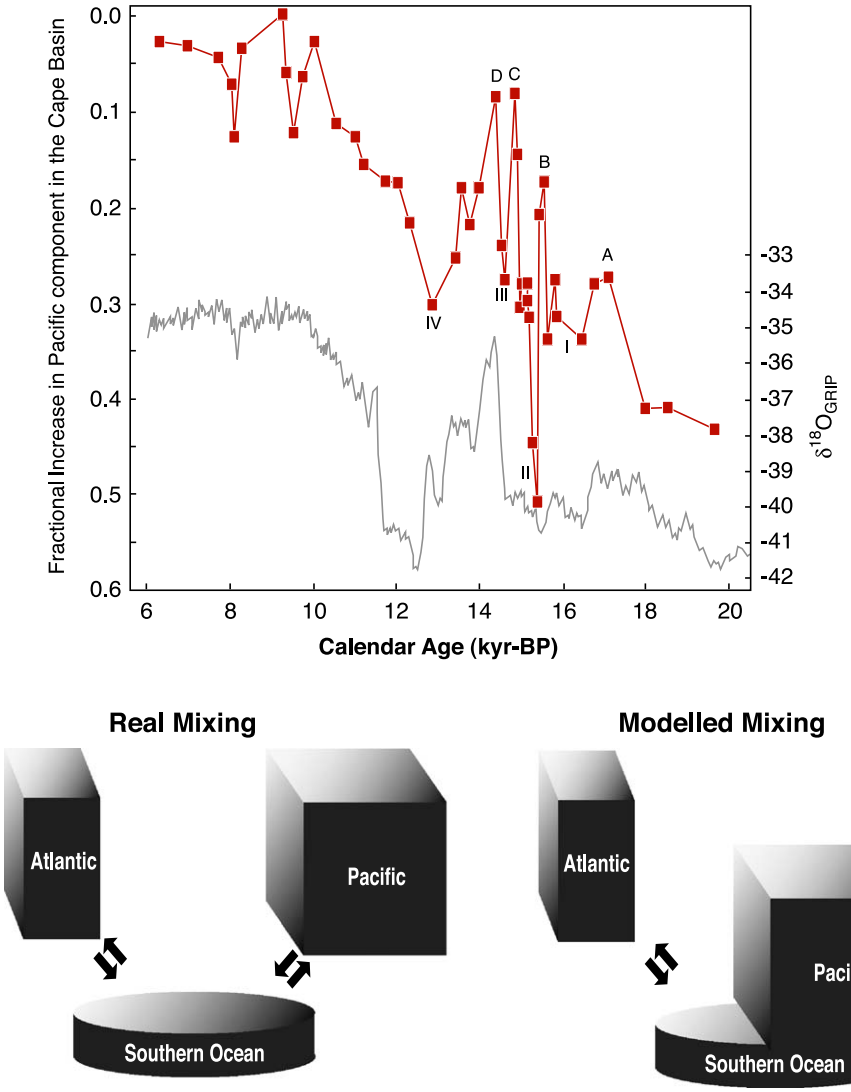

Fig. 4. Changes in NADW signal to RC11-83 through the deglaciation. Nd isotope record expressed as fractional increase in the Pacific component in RC11-83. In this calculation, the NADW end-member is assigned $\varepsilon_{Nd} = -14$, Nd concentration of 17 pmol/kg for NADW [25], while the Pacific end-member assigned is $\varepsilon_{Nd} = -4$, Nd concentration of 40 pmol/kg. The values are normalized to the largest NADW signal which is observed in the early Holocene. As the estimate reflects the changes in the Pacific signal, as illustrated in the lower panel, it is not an estimate of the Southern Ocean–NADW mixing.

water ($\varepsilon_{Nd} = -3$ to -4) contrast sharply with low values in the continent-derived detritus ($\varepsilon_{Nd} \sim -10$) [67,68]. As discussed in Section 4, currently available data on Fe–Mn crusts and nodules justify the assumption of constancy of the North Atlantic and Pacific end-members through the late Pleistocene, and in the Pacific, this is further supported by evidence from manganiferous carbonate sediments. These observations justify a first attempt at a mass balance based on this assumption.

Secondly, we assume that local detrital inputs to the South Atlantic do not significantly affect deep-water Nd isotope ratios. This is supported by studies showing that the seawater Nd isotope ratios in depth profiles in the North and South Atlantic vary with water mass [26,69], that Nd in sinking

particles do not appear to exchange with deep water [25,70], and correlated Nd isotope ratios and SiO_2 in deep Atlantic seawater, indicating that Nd isotope ratios conservatively reflect mixing of water masses [25].

Thirdly, the mass balance uses the Pacific rather than the Southern Ocean as an end-member (Fig. 4, lower panel), and thus is an estimate of the relative change in the strengths of the North Atlantic and Pacific signals through time. The Nd isotopic signature of the Southern Ocean during this time interval is poorly constrained by published data, although measurements on TNO57-6 by Rutberg et al. [17] and this paper (Table 1) indicate that during the LGM it was close to the composition of the Pacific, suggesting a greatly reduced NADW contribution to the Southern Ocean.

Our estimate of NADW variability (Fig. 4) is plotted relative to the early Holocene maximum. While the temporal pattern is similar to that of Nd isotopes versus age (Figs. 2 and 3), it accounts for the lower Nd abundances in North Atlantic relative to Pacific seawater. The estimate indicates that the Pacific component reaching RC11-83 was ~40% stronger during Older Dryas the LGM and ~30% stronger during the Younger Dryas, compared to the early Holocene. The weakest NADW signal (trough II) follows the "NADW false start" of Charles and Fairbanks [6] (peak B), corresponding to a 50% increase in the Pacific component. During the Bølling NADW peak and the one immediately preceding it (D and C, respectively), NADW intensity reaches near Holocene levels, with the Pacific component only ~5% stronger than during the early Holocene minimum, while during Older Dryas peaks B and A, the Pacific component was ~15% and 25% stronger, respectively, than during the early Holocene NADW. Thus, it appears that as the termination progressed, along with the increasing baseline strength of the NADW signal, the maximum strength of the NADW signal during millennial peaks also tended to increase.

10. Conclusions

Our Nd isotope record of NADW transport to the Southern Ocean through the last deglaciation indicates a gradually increasing baseline intensity for the global overturning circulation beginning approximately between 18 and 17 kyr cal. BP, a few thousand years prior to the Bølling warming, tracking increasing Northern hemisphere insolation. Superimposed on the baseline increase are rapid millennial fluctuations in NADW production, which are tied to climate changes in the circum-North Atlantic. Following each excursion, the NADW intensity returned to the baseline level. The gradually increasing baseline through the deglaciation indicates that thermohaline circulation does not switch between distinct glacial and interglacial modes of circulation but rather that varies as a continuum. On the other hand, the abrupt changes necessitate the existence of mechanisms capable of rapid strengthening and weakening thermohaline circulation intensity on millennial timescales. Sea ice, capable of rapidly responding to integrated changes in atmospheric and surface ocean circulation, likely transmitted this pattern of abrupt climate change to the deep ocean by constraining the latitude of NADW formation sites. The baseline NADW increase in our record may reflect the progressive northward shift of the sea ice edge in response to increasing insolation during the deglaciation. In addition, the covariation of rapid fluctuations of NADW strength and sea ice coverage in the North Atlantic suggests that sea ice extent acts as an important amplifying link between thermohaline circulation and rapid shifts in atmospheric circulation. Altogether, the data suggest a strong link between the baseline global overturning circulation intensity and Milankovitch forcing, with abrupt changes reflecting North Atlantic regional climate and sea ice coverage.

Acknowledgements

This manuscript benefited from discussions with R. Anderson, G. Bond, W. Broecker, M. Cane, D. Hodell, D. Martinson, R. Rutberg, R. Seager, and S. Zimmerman. We appreciate reviews by Germain Bayon, Martin Frank, and an anonymous referee whose comments have led to improvements in the manuscript. AMP thanks M. Klas-Mendelsohn and H. Kushnir for help in the lab. Samples were provided by the LDEO Deep-Sea Sample Repository, which is supported by the National Science Foundation (Grant OCE00-02380) and the Office of Naval Research

(Grant N00014-02-1-0073). The Nd and Sr isotopic measurements were supported by NSF grants OCE 98-09253 and OCE 00-96427 to SLG and SRH. The new radiocarbon dates were supported by NOAA CORC-ARCHES grant 10196097 to SRH and SLG and OCE 98-18349 and OCE 99-11637 to RGF. This is LDEO Contribution #6638.

References

[1] P.K. Weyl, The role of ocean circulation in climatic changes: a theory of ice ages, Meteorological Monographs 8 (1968) 37–62.
[2] W.S. Broecker, G.H. Denton, The role of ocean-atmosphere reorganizations in Glacial Cycles, Geochimica et Cosmochimica Acta 53 (10) (1989) 2465–2501.
[3] A.C. Clement, M.A. Cane, R. Seager, An orbitally driven tropical source for abrupt climate change, Journal of Climate 14 (11) (2001) 2369–2375.
[4] A.C. Mix, R.G. Fairbanks, North-Atlantic surface-ocean control of Pleistocene deep-ocean circulation, Earth and Planetary Science Letters 73 (2–4) (1985) 231–243.
[5] D.W. Oppo, R.G. Fairbanks, Variability in the deep and intermediate water circulation of the Atlantic-ocean during the past 25,000 years—Northern-Hemisphere modulation of the southern-ocean, Earth and Planetary Science Letters 86 (1) (1987) 1–15.
[6] C.D. Charles, R.G. Fairbanks, Evidence from southern-ocean sediments for the effect of North-Atlantic deep-water flux on climate, Nature 355 (6359) (1992) 416–419.
[7] E.F. Yu, R. Francois, M.P. Bacon, Similar rates of modern and last-glacial ocean thermohaline circulation inferred from radiochemical data, Nature 379 (6567) (1996) 689–694.
[8] D.W. Lea, A trace-metal perspective on the evolution of Antarctic circumpolar deep-water chemistry, Paleoceanography 10 (4) (1995) 733–747.
[9] E.A. Boyle, Glacial interglacial deep ocean circulation contrast, Chemical Geology 70 (1–2) (1988) 108.
[10] C.D. Charles, J.D. Wright, R.G. Fairbanks, Thermodynamic influences on the marine carbon-isotope record, Paleoceanography 8 (6) (1993) 691–697.
[11] J. Lynch-Stieglitz, T.F. Stocker, W.S. Broecker, R.G. Fairbanks, The influence of air-sea exchange on the isotopic composition of oceanic carbon—observations and modeling, Global Biogeochemical Cycles 9 (4) (1995) 653–665.
[12] A. Mackensen, H.W. Hubberten, T. Bickert, G. Fischer, D.K. Futterer, The Delta-C-13 in benthic foraminiferal tests of Fontbotia–Wuellerstorfi (Schwager) relative to the Delta-C-13 of dissolved inorganic carbon in southern-ocean deep-water—implications for glacial ocean circulation models, Paleoceanography 8 (5) (1993) 587–610.
[13] D.C. McCorkle, P.A. Martin, D.W. Lea, G.P. Klinkhammer, Evidence of a dissolution effect on benthic foraminiferal shell chemistry—Delta-C-13, Cd/Ca, Ba/Ca, and Sr/Ca results from the Ontong Java Plateau, Paleoceanography 10 (4) (1995) 699–714.
[14] T.M. Marchitto, W.B. Curry, D.W. Oppo, Zinc concentrations in benthic foraminifera reflect seawater chemistry, Paleoceanography 15 (3) (2000) 299–306.
[15] O. Marchal, R. Francois, T.F. Stocker, F. Joos, Ocean thermohaline circulation and sedimentary Pa-231/Th-230 ratio, Paleoceanography 15 (6) (2000) 625–641.
[16] T. Asmus, M. Frank, C. Koschmieder, N. Frank, R. Gersonde, G. Kuhn, A. Mangini, Variations of biogenic particle flux in the southern Atlantic section of the sub-Antarctic zone during the late quaternary: evidence from sedimentary Pa-231(ex) and Th-230(ex), Marine Geology 159 (1–4) (1999) 63–78.
[17] R.L. Rutberg, S.R. Hemming, S.L. Goldstein, Reduced North Atlantic deep water flux to the glacial southern ocean inferred from neodymium isotope ratios, Nature 405 (6789) (2000) 935–938.
[18] G. Bayon, C.R. German, R.M. Boella, J.A. Milton, R.N. Taylor, R.W. Nesbitt, An improved method for extracting marine sediment fractions and its application to Sr and Nd isotopic analysis, Chemical Geology 187 (2002) 179–199.
[19] D.J. Piepgras, G.J. Wasserburg, E.J. Dasch, Isotopic composition of Nd in different ocean masses, Earth and Planetary Science Letters 45 (2) (1979) 223–236.
[20] D.J. Piepgras, G.J. Wasserburg, Neodymium isotopic variations in seawater, Earth and Planetary Science Letters 50 (1) (1980) 128–138.
[21] S.L. Goldstein, R.K. O'Nions, Nd and Sr isotopic relationships in pelagic clays and ferromanganese deposits, Nature 292 (5821) (1981) 324–327.
[22] M.C. Stordal, G.J. Wasserburg, Neodymium isotopic study of Baffin-bay water—sources of REE from very old terranes, Earth and Planetary Science Letters 77 (3–4) (1986) 259–272.
[23] F. Albarède, S.L. Goldstein, World map of Nd isotopes in seafloor ferromanganese deposits, Geology 20 (1992) 761.
[24] M. Frank, Radiogenic isotopes: tracers of past ocean circulation and erosional input, Reviews of Geophysics 40 (1) (2002) 1–38.
[25] S.L. Goldstein, S.R. Hemming, Long-lived isotopic tracers in oceanography, paleoceanography and ice sheet dynamics, in: H. Elderfield (Ed.), Treatise on Geochemistry, vol. 6Elsevier, Oxford, 2003, pp. 453–489.
[26] C. Jeandel, Concentration and isotopic composition of Nd in the South-Atlantic ocean, Earth and Planetary Science Letters 117 (3–4) (1993) 581–591.
[27] M.R. Palmer, H. Elderfield, Rare earth elements and neodymium isotopes in ferromanganese oxide coatings of Cenozoic foraminifera from the Atlantic Ocean, Geochimica Cosmochimica Acta 50 (1986) 409–417.
[28] K.W. Burton, D. Vance, Glacial-interglacial variations in the neodymium isotope composition of seawater in the Bay of Bengal recorded by planktonic foraminifera, Earth and Planetary Science Letters 176 (3–4) (2000) 425–441.
[29] C.D. Charles, J. Lynch-Stieglitz, U.S. Ninnemann, R.G. Fair-

banks, Climate connections between the hemispheres revealed by deep sea sediment core ice core correlations, Earth and Planetary Science Letters 142 (1–2) (1996) 19–27.
[30] S. Levitus, R. Burgett, T. Boyer, World Ocean Atlas 1994: Nutrients, U.S. Department of Commerce, Washington, DC, 1994.
[31] M. Stuiver, P.J. Reimer, E. Bard, J.W. Beck, G.S. Burr, K.A. Kromer, B. Kromer, G. McCormac, J. Van der Plicht, M. Spurk, INTCAL98 radiocarbon age calibration, 24,000-0 cal BP, Radiocarbon 40 (3) (1998) 1041–1083.
[32] E. Bard, M. Arnold, B. Hamelin, N. Tisnerat-Laborde, G. Cabioch, Radiocarbon calibration by means of mass spectrometric Th-230/U-234 and C-14 ages of corals: an updated database including samples from Barbados, Mururoa and Tahiti, Radiocarbon 40 (3) (1998) 1085–1092.
[33] R.L. Rutberg, S.L. Goldstein, S.R. Hemming, Agulhas leakage variability from Sr isotopes in south Atlantic detritus, Geochimica Et Cosmochimica Acta 66 (15A) (2002) A658.
[34] W. Abouchami, S.L. Goldstein, S.J.G. Galer, A. Eisenhauer, A. Mangini, Secular changes of lead and neodymium in Central Pacific seawater recorded by a Fe–Mn crust, Geochimica Et Cosmochimica Acta 61 (18) (1997) 3957–3974.
[35] R. Oxburgh, S.R. Hemming, Pleistocene Nd and Os isotope variations in sediments from the East Pacific rise, EOS 77 (1996) F324.
[36] A. Berger, M.F. Loutre, Insolation values for the climate of the last 10,000,000 years, Quaternary Science Reviews 10 (4) (1991) 297–317.
[37] H.J. Smith, H. Fischer, M. Wahlen, D. Mastroianni, B. Deck, Dual modes of the carbon cycle since the Last Glacial Maximum, Nature 400 (6741) (1999) 248–250.
[38] A. de Vernal, C. Hillaire-Marcel, Sea-ice cover, sea-surface salinity and halo-/thermocline structure of the northwest North Atlantic: modern versus full glacial conditions, Quaternary Science Reviews 19 (1–5) (2000) 65–85.
[39] A. de Vernal, M. Henry, J. Matthiessen, P.J. Mudie, A. Rochon, K.P. Boessenkool, F. Eynaud, K. Grosfjeld, J. Hamel, D. Hamel, R. Harland, M.J. Head, M. Kunz-Pirrung, E. Levac, V. Loucheur, O. Peyron, V. Pospelova, T. Radi, J.L. Turon, E. Voronina, Dinoflagellate cyst assemblages as tracers of sea-surface conditions in the northern North Atlantic, Arctic and sub- Arctic seas: the new '$n=677$' data base and its application for quantitative palaeoceanographic reconstruction, Journal of Quaternary Science 16 (7) (2001) 681–698.
[40] G.H. Denton, C.J. Heusser, T.V. Lowell, P.I. Moreno, B.G. Andersen, L.E. Heusser, C. Schluchter, D.R. Marchant, Interhemispheric linkage of paleoclimate during the last glaciation, Geografis Ka Annaler. Series A. Physical Geography 81A (2) (1999) 107–153.
[41] S.J. Lehman, L.D. Keigwin, Sudden changes in North-Atlantic circulation during the last deglaciation, Nature 356 (6372) (1992) 757–762.
[42] J. Kutzbach, Model simulations of the climatic patterns during the deglaciation of North America, in: W.F. Ruddiman, H.E. Wright (Eds.), North America and Adjacent Oceans During the Last Deglaciation, The Geology of North America vol. K-3, Geological Society of America, Boulder, CO, 1987, pp. 425–446.
[43] C.D. Charles Jr., D. Rind, J. Jouzel, R.D. Koster, R.G. Fairbanks, Glacial-interglacial changes in moisture sources for Greenland—influences on the ice core record of climate, Science 263 (5146) (1994) 508–511.
[44] J.F. Adkins, H. Cheng, E.A. Boyle, E.R.M. Druffel, R.L. Edwards, Deep-sea coral evidence for rapid change in ventilation of the deep North Atlantic 15,400 years ago, Science 280 (5364) (1998) 725–728.
[45] G. Bond, W. Broecker, S. Johnsen, J. Mcmanus, L. Labeyrie, J. Jouzel, G. Bonani, Correlations between climate records from North-Atlantic sediments and Greenland Ice, Nature 365 (6442) (1993) 143–147.
[46] J.F. McManus, R. Francois, J.-M. Gherardi, L. Keigwin, S. Brown-Leger, Collapse and rapid resumption of Atlantic meridional circulation linked to deglacial climate changes, Nature 428 (2004) 834–837.
[47] W.F. Ruddiman, A. Mcintyre, The North-Atlantic ocean during the last deglaciation, Palaeogeography, Palaeoclimatology, Palaeoecology 35 (2–4) (1981) 145–214.
[48] M. Elliot, L. Labeyrie, G. Bond, E. Cortijo, J.L. Turon, N. Duplessy, J.C. Duplessy, Millennial-scale iceberg discharges in the Irminger Basin during the last glacial period: relationship with the Heinrich events and environmental settings, Paleoceanography 13 (5) (1998) 433–446.
[49] R.G. Fairbanks, A 17,000-year Glacio-Eustatic Sea-level record—influence of glacial melting rates on the Younger Dryas event and deep-ocean circulation, Nature 342 (6250) (1989) 637–642.
[50] D. Rind, P. deMenocal, G. Russell, S. Sheth, D. Collins, G. Teller, J. Teller, Effects of glacial meltwater in the GISS coupled atmosphere ocean model: 1. North Atlantic deep water response, Journal of Geophysical Research—Atmospheres 106 (D21) (2001) 27335–27353.
[51] S. Manabe, R.J. Stouffer, Simulation of abrupt climate-change induced fresh-water input to the North Atlantic Ocean, Nature 378 (6553) (1995) 165–167.
[52] H. Gildor, E. Tziperman, Sea-ice switches and abrupt climate change, Philosophical Transactions of the Royal Society of London, Series A: Mathematical and Physical Sciences 361 (1810) (2003) 1935–1942.
[53] R.G. Fairbanks, C.D. Charles, J.D. Wright, Origin of global meltwater pulses, in: A. Long, R.S. Kra (Eds.), Radiocarbon After Four Decades: An Interdisciplinary Perspective, Springer, 1992, pp. 473–500.
[54] W.B. White, R.G. Peterson, An Antarctic circumpolar wave in surface pressure, wind, temperature and sea-ice extent, Nature 380 (6576) (1996) 699–702.
[55] R. Kwok, D.A. Rothrock, Variability of Fram Strait ice flux and North Atlantic Oscillation, Journal of Geophysical Research—Oceans 104 (C3) (1999) 5177–5189.
[56] R. Hilmer, M. Harder, P. Lemke, Sea ice transport: a highly variable link between Arctic and North Atlantic, Geophysical Research Letters 25 (17) (1998) 3359–3362.
[57] M. Hilmer, T. Jung, Evidence for a recent change in the

link between the North Atlantic Oscillation and Arctic sea ice export, Geophysical Research Letters 27 (7) (2000) 989–992.
[58] J. Marshall, Y. Kushner, D. Battisti, P. Chang, A. Czaja, R. Hurrell, J. Hurrell, M. McCartney, R. Saravanan, M. Visbeck, North Atlantic climate variability: phenomena, impacts and mechanisms, International Journal of Climatology 21 (15) (2001) 1863–1898.
[59] B. Dickson, J. Meincke, I. Vassie, J. Jungclaus, S. Osterhus, Possible predictability in overflow from the Denmark Strait, Nature 397 (6716) (1999) 243–246.
[60] R. Seager, D.S. Battisti, J. Yin, N. Gordon, N. Naik, A.C. Cane, M.A. Cane, Is the Gulf Stream responsible for Europe's mild winters? Quarterly Journal of the Royal Meteorological Society 128 (586) (2002) 2563–2586.
[61] O. Marchal, T.F. Stocker, R. Muscheler, Atmospheric radiocarbon during the Younger Dryas: production, ventilation, or both? Earth and Planetary Science Letters 185 (3–4) (2001) 383–395.
[62] T.F. Stocker, D.G. Wright, Rapid changes in ocean circulation and atmospheric radiocarbon, Paleoceanography 11 (6) (1996) 773–795.
[63] S. Rahmstorf, Rapid climate transitions in a coupled ocean–atmosphere model, Nature 372 (6501) (1994) 82–85.
[64] K. Tachikawa, V. Athias, C. Jeandel, Neodymium budget in the modern ocean, paleo-oceanographic implications, Journal of Geophysical Research—Oceans 108 (C8)(Art. No. 3254).
[65] C. Innocent, N. Fagel, R.K. Stevenson, C. HillaireMarcel, Sm–Nd signature of modern and late Quaternary sediments from the northwest North Atlantic: implications for deep current changes since the last glacial maximum, Earth and Planetary Science Letters 146 (3–4) (1997) 607–625.
[66] N. Fagel, C. Innocent, R.K. Stevenson, C. Hillaire-Marcel, Deep circulation changes in the Labrador Sea since the last glacial maximum: new constraints from Sm–Nd data on sediments, Paleoceanography 14 (6) (1999) 777–788.
[67] S. Nakai, A.N. Halliday, D.K. Rea, Provenance of dust in the Pacific-Ocean, Earth and Planetary Science Letters 119 (1–2) (1993) 143–157.
[68] C.E. Jones, A.N. Halliday, D.K. Rea, R.M. Owen, Neodymium isotopic variations in North Pacific modern silicate sediment and the insignificance of detrital REE contributions to seawater, Earth and Planetary Science Letters 127 (1994) 55–66.
[69] D.J. Piepgras, G.J. Wasserburg, Rare-earth element transport in the Western North-Atlantic inferred from Nd isotopic observations, Geochimica Et Cosmochimica Acta 51 (5) (1987) 1257–1271.
[70] C. Jeandel, J.K. Bishop, A. Zindler, Exchange of neodymium and its isotopes between seawater and small and large particles in the Sargasso Sea, Geochimica Et Cosmochimica Acta 59 (3) (1995) 535–547.
[71] S.B. Jacobsen, G.J. Wasserburg, Sm–Nd isotopic evolution of chondrites 50 (1) (1980) 139–155.
[72] G.J. GRIP_Members, Climate instability during the last interglacial period recorded in the GRIP ice core, Nature 364 (1993) 203–207.
[73] S.J. Johnsen, H.B. Clausen, W. Dansgaard, N.S. Gundestrup, C.U. Hammer, U. Andersen, K.K. Andersen, C.S. Hvidberg, D. Dahl-Jensen, J.P. Steffensen, H. Shoji, A.E. White, J.W.C. White, J. Jouzel, D. Fisher, The $\delta^{18}O$ record along the Greenland Ice Core Project deep ice core and the problem of possible Eemian climatic instability, Journal of Geophysical Research 102 (1997) 26397–26410.